C.E. SACLAY
DSM

SERVICE DE PHYSIQUE NUCLÉAIRE

DAPNIA-SPhN-96-11 04/1996

$^{35}Cl + {}^{12}C$ Asymmetrical Fission Excitation Functions

C. Beck, D. Mahboub, R. Nouicer, T. Matsuse, B. Djerroud, R.M. Freeman, F. Haas, A. Hachem, A. Morsad, M. Youlal, S.J. Sanders, R. Dayras, J.P. Wieleczko, E. Berthoumieux, R. Legrain, E. Pollacco, Sl. Cavallaro, E. de Filippo, G. Lanzano, A. Pagano and M.L. Sperduto

DAPNIA

Le DAPNIA (**D**épartement d'**A**strophysique, de physique des **P**articules, de physique **N**ucléaire et de l'**I**nstrumentation **A**ssociée) regroupe les activités du Service d'Astrophysique (SAp), du Département de Physique des Particules Elémentaires (DPhPE) et du Département de Physique Nucléaire (DPhN).

Adresse : DAPNIA, Bâtiment 141
CEA Saclay
F -91191 Gif-sur-Yvette Cedex

The Physical Review C

$^{35}Cl+^{12}C$ ASYMMETRICAL FISSION EXCITATION FUNCTIONS

C. Beck, D. Mahboub, R. Nouicer, T. Matsuse[a], B. Djerroud[b], R.M. Freeman, F. Haas, A. Hachem[c], A. Morsad[d] and M. Youlal

Centre de Recherches Nucléaires, Institut National de Physique Nucléaire et de Physique des Particules - Centre National de la Recherche Scientifique/Université Louis Pasteur,B.P.28, F-67037 Strasbourg Cedex 2, France

S.J. Sanders

The University of Kansas, Department of Physics and Astronomy, Lawrence KS 66045, USA

R. Dayras, J.P. Wieleczko[e], E. Berthoumieux, R. Legrain, E. Pollacco

DAPNIA/SPhN, C.E. Saclay, F-91191 Gif sur Yvette Cedex, France

Sl. Cavallaro, E. De Filippo, G. Lanzanò, A. Pagano and M.L. Sperduto

Dipartimento di Fisica dell'Universitá di Catania, INFN and LNS Catania, I-95129 Catania, Italy

(March 7, 1996)

Abstract

The fully energy-damped yields from the $^{35}Cl+^{12}C$ reaction have been systematically investigated using particle-particle coincidence techniques at a ^{35}Cl bombarding energy of $\sim$ 8 MeV/nucleon. The fragment-fragment correlation data show that the majority of events arises from a binary-decay process with rather large numbers of secondary light-charged particles emitted from the two excited exit fragments. No evidence is observed for ternary break-up events. The binary-process results of the present measurement, along with those of earlier, inclusive experimental data obtained at several lower bombarding energies are compared with predictions of two different kinds of statistical model calculations. These calculations are performed using the transition-state formalism and the Extended Hauser-Feshbach method and are based on the available phase space at the saddle point and scission point of the compound nucleus, respectively. The methods give comparable predictions and are both in good agreement with the experimental results thus confirming the fusion-fission origin of the fully-damped yields. The similarity of the predictions for the two models supports the claim that the scission point configuration is very close to that of the saddle point for the light ^{47}V compound system. The results also give further support for the specific mass-asymmetry-dependent fission barriers needed in the transition-state calculation.

PACS numbers: 25.70.Jj, 24.60.Dr, 25.70.Gh, 25.70.-z

I. INTRODUCTION

The $^{35}Cl+^{12}C$ binary-reaction channels have been studied over the past few years [1–3] at several relatively low ^{35}Cl bombarding energies ($E_{lab} \leq 200$ MeV), in the framework of a more general investigation of the ^{47}V composite system [3–5]. It has been established that entrance channel effects do not play a significant role in the binary-decay processes of the ^{47}V nucleus as populated by the three studied entrance channels ($^{35}Cl+^{12}C$ [1,2], $^{31}P+^{16}O$ [4] and $^{23}Na+^{24}Mg$ [5]) at comparable excitation energies (E^*_{CN} = 59-64 MeV) and angular momenta. This demonstrates that in each case the compound nucleus (CN) is formed after a complete equilibration of the mass asymmetry and the shape degrees of freedom. Further, the properties of the binary-decay channels are in agreement with the expectations of the transition-state model [6] and thus suggest a fusion-fission (FF) origin. The occurrence of FF rather than orbiting in certain systems, such as the ^{47}V dinucleus, has been the subject of large number of discussions [2–9]. These have led, in most cases, to the conclusion that the FF process has to be taken into account when exploring the limitations of the complete fusion process at large angular momenta and high excitation energies. This is in accordance with the qualitative expectations of the number of open channels model [10].

In this paper we report on further inclusive measurements on FF yields of $^{35}Cl+^{12}C$ at a bombarding energy $E_{lab}(^{35}Cl) = 280$ MeV. This significantly extends the known complete FF excitation function for this reaction. In addition, fragment-fragment correlation data have been collected to check the relative importance of mechanisms other than secondary particle emission for the high excitation energy ($E^*_{CN} = 85$ MeV) in the compound system reached by this reaction. Light-fragment emission from the reaction fragments can lead to a "charge deficit" between the observed and entrance-channel charge. The charge deficits in the present measurement are extracted from the coincidence data in order to verify that they follow the systematic trend that has been found with previously published results, thus confirming the binary nature of the reaction. No evidence is seen for the onset of ternary

processes for incident energies lower than 10 MeV/nucleon.

It is known that the secondary and sequential light-charged-particle emission from the fully accelerated binary-decay fragments increases with energy. Nevertheless, the properties of the primary fission fragments can be deduced, even at energies as high as 280 MeV, by using the coincident data. As found at the lower energies studied [1–3] the hypothesis of CN formation followed by a statistical decay is supported by the present data. Further, the measured FF excitation function for each fragment atomic number is found to be compatible with the choice of mass-asymmetric-dependent fission barriers used in the transition-state model calculations [6].

A brief description of the experimental techniques is given in the next section. The experimental results of the single and coincidence measurements are presented in Sect.III. These results are then discussed in Sect.IV within the framework of two distinctly different FF pictures based upon whether the saddle point [6] or the scission point [7,8] determines the fission decay rates.

II. EXPERIMENTAL PROCEDURES

The investigation of the $^{35}Cl+^{12}C$ reaction has been achieved at the Strasbourg 18 MV MP Tandem and the Saclay Booster Tandem facilities by means of kinematical coincidence techniques. Further details of the experimental methods can be found elsewhere [2,3,5] in the experimental descriptions for the lower energy measurements. The experiments at the highest energy were performed with the 278-280 MeV pulsed beams, provided by the Saclay post-accelerator, focused onto a 100 $\mu g/cm^2$ thick, self-supporting ^{12}C target mounted at the center of the 2 meter wide scattering chamber "chambre 2000". Some data which will be presented in the discussion were also recorded with a 255 $\mu g/cm^2$ thick ^{24}Mg target for

a study of the $^{35}Cl+^{24}Mg$ reaction [9]. During the course of the experiment at 280 MeV the reaction products were detected, in a singles mode, either with four small size ΔE-E telescopes (located in the 10°-350 angular range with a 2° step increment), each consisting of a gas ionization chamber followed by a 500 μm thick Si(SB) detector (IC), or with a large size, movable, Bragg Curve Spectrometer (BCS) [11] covering the 2.5°-12" angular range with 1° steps. The experimental set-up for the coincidence experiment at E_{lab} = 278 MeV was very similar to that used for the inclusive experiment and consisted of seven ionization-chamber telescopes in the reaction plane between - 37° and + 85°.

The energy calibrations of the BCS and IC's were obtained using elastically scattered ^{35}Cl projectiles from a 100 $\mu g/cm^2$ thick Au target and from the C and Mg targets, combined with measurements of α sources and a calibration pulser. On an event-by-event basis, corrections were applied for energy loss in the target and IC's window foils and for the pulse height defect in the Si detectors [12]. The absolute normalization of the measured differential cross sections was determined from an optical model analysis of the elastic scattering measured at the more forward angles using potential parameters found to fit accurately the lower energy data for the same reaction [2].

A typical two-dimensional charge (Z) versus velocity (v) contour plot of the fragment invariant cross sections is given in Fig. 1 for θ_{lab} = - 7°. The velocity v has been deduced by using the empirical mass formula of Charity and collaborators [13] on the basis of an event-by-event analysis. Three distinct zones can be clearly identified. The first, where Z is close to that of the projectile (Z = 17), corresponds to the quasi-elas tic group having a mean velocity close to that of the projectile (VP). For higher Z ($Z \geq 18$) the fragment velocities are well centered around the CN recoil velocity (v_{CN}) and thus correspond to fusion-evaporation residues (ER). The third class of events is distributed on two, well separated velocity branches which merge together as Z is increased, as expected for binary-decay processes in a reverse kinematics reaction. It is observed that the two branches which correspond to the two allowed kinematic solutions, overlap gradually as the detection angles are increased. The two groups belonging to the second solution arise either from asymmetric-

fission components ($6 \leq Z \leq 10$) or from symmetric-fission components which are mixed with deep-inelastic (DI) collisions events ($11 \leq Z \leq 15$) with large mass transfer.

In the following, the properties of the binary fragments belonging to this last class of events will be discussed in detail. These fragments arise from fully energy-damped reactions. This fact is illustrated by the solid lines drawn in Fig.1 which have been calculated by using the Viola systematic [14] for symmetric-fission fragments. The velocities of the non-symmetric mass fragments have been corrected by the following asymmetric factor [15,3]: $4Z_1Z_2/(Z_1+Z_2)^2$, where $Z_{1,2}$ are the charges of the outgoing fragments.

III. EXPERIMENTAL RESULTS

Inclusive kinetic energy spectra were measured for each Z fragment produced in the $^{35}Cl+^{12}C$ reaction at E_{lab} = 278 MeV and presented in Fig.2 for θ_{lab} = - 7°. The heaviest fragments belonging to the second zone, discussed in the previous section and displayed in Fig.1, have typical ER energy spectra arising from the statistical decay of the fully equilibrated CN formed in a complete fusion process. This is confirmed by the excellent agreement found for ER with $Z \geq 18$ with the expectations of the Monte Carlo code LILITA [17] as shown by the black histograms of Fig.2. It is worth noting that, according to the fusion systematic of Morgenstern and collaborators [16], less than 5 % of the observed ER yield is expected to arise from an incomplete fusion process. The ER components of the $14< Z \leq 17$ energy spectra have been extracted from other binary-reaction components (yields have been generated by a model to be discussed in Sect. IV) with the aid of the LILITA simulations at each angle. The energy spectra of the lightest of the fragments ($5 \leq Z \leq 12$) are dominated by the third class of events discussed in the preceding section and have typical characteristic Gaussian shapes whose centroids correspond to binary breakup with

full energy damping, consistent with the Viola systematic [14]. The increasing yields at low energy, near the experimental energy threshold, arise from the second allowed kinematic solution.

The centroids of the first kinematic solution have been extracted for each Z in order to deduce their total kinetic energy (TKE) values assuming two-body kinematics in the center-of-mass (cm.) frame. The results are shown in Fig.3. The dependence of the TKE's and of the differential cross sections $d\sigma/d\theta$ (not shown) on the scattering angle for each exit channel indicate that the lifetime of the dinuclear complex is longer than the time needed to fully damp the energy in the relative motion of FF and DI processes. The average TKE values, also plotted in the insert of Fig.3 as a function of Z, are found to be very close to the values extracted at lower incident energies [1,2], with only small variations with the incident energy, in contrast to what can be expected for a DI orbiting mechanism [18]. The dashed line is the result of a calculation of the equilibrium model for orbiting [18] with the parameter set used previously at lower bombarding energies [2]. The large discrepancies are essentially due to an overestimation of the TKE rotational term induced by neglecting diffuse-surface effects in the calculations performed without corrections for secondary light-particle emission. On the other hand, the results of FF model predictions (which will be discussed in the following section), including both these effects, are shown by the solid line to be very close to the mean values of experimental data. Furthermore the average TKE value corresponding to symmetric mass splitting is close to the prediction of Viola [14] and to that of more recent systematic well suited for light heavy-ions [19].

The experimental elemental Z distribution (full points) of the integrated fully-damped yields (for $Z \leq 12$) and ER cross sections are plotted in Fig.4 with two statistical model calculations (histograms) which will be discussed in detail in the next section. Because of the potential mixing with large DI components (which might be composed of either partially or fully-damped yields), no attempt has been make to extract the FF yields for Z = 13 and 14. The total FF and ER cross sections are σ_{FF} = 25.0 ± 4.5 mb and σ_{ER} = 763 ± 100 mb respectively. The corresponding critical angular momentum is $L_{crit} = 27.5 \pm 2.5\,\hbar$

as calculated by using the sharp cutoff approximation. This value is taken as an input parameter for the statistical model calculations discussed in the next section.

The possible occurrence of ternary processes that involve three massive fragments in competition with the binary-decay mechanisms has been searched for in the fragment-fragment coincidence experiment. The angular correlations obtained are displayed in Fig.5 for the indicated charge partitions and angle settings. They are found to peak at well defined angles between θ_2 = 30° and 50°, independent of the charge partition, indicating that the fragments have a dominant two-body nature as expected for energies lower than 10 MeV/nucleon [20-22]. The peak positions in the correlation functions are a measure of the reaction Q-value for the primary decay. As an example the large and narrow peak for Z_1=17 and Z_2=6 has the position expected for the elastic scattering, whereas the second and smaller peak at 55° might correspond to a fast neutron transfer process. Similar narrow peaks are observed at comparable angles in other correlations with (Z_1=17 and Z_2=5) and (Z_1=16 and Z_2=6) that may be attributed to quasielastic proton stripping or pick-up processes. More fully-damped processes have larger width correlations which are peaked at smaller angles. The role of secondary light-particle emission will be to broaden these distributions, but without significantly affecting the centroids of the correlations.

In previous experiments using projectiles of mass A_{proj} = 32 to 40 on various targets, events corresponding to the emission of three heavy fragments (A $\geq$ 5) have been found to occur significantly (at a 10 % level) only at higher bombarding energies (10-15 MeV/nucleon) [23-25]. More recently, however, there has been evidence cited in the literature [26,27] for three-body events in ^{32}S induced reactions at lower energies (4-6 MeV/nucleon).

In the following we investigate this possibility of three fragment emission in the present exclusive data through the analysis of the 2_1-2_2 coincident yields which have been energy integrated for $Z_{1,2} \geq 5$. The Z_1-Z_2 correlation results are displayed in Fig.6 for the indicated angle settings. The diagonal lines given by $Z_1+Z_2 = Z_{proj}+Z_{target} = Z_{CN}$ = 23 correspond to binary reactions with no light-charged-particle evaporation. The majority of events are found to occur near Z_{tot} = 20-21, regardless of whether the exit-mass partition is symmetric

or not. Thus the most probable missing charge ΔZ was found to be around 2 charge units, which is most likely lost through particle emission from either the excited composite system or a secondary sequential evaporation from one of the binary-reaction partners. In order to perform a more quantitative analysis of these processes we have plotted in Fig.7 and Fig.8 the coincident yields as a function of the missing charge for the chosen angle settings. These results are discussed in the next section.

IV. **DISCUSSION** AND CONCLUSION

The spectra of the summed missing charge, displayed in Fig.7, have typical Poisson-like distributions with most probable value $\lambda = < \Delta Z >$:

$$P(\Delta Z) \propto \lambda^{\Delta Z} e^{-\lambda} / \Delta Z!$$

The corresponding fits by using this expression are also given in the figure. The angular dependence of the maxima gives an estimate of the energy transferred into the fragments according to the two-body kinematics. It should be noted that a non-statistical emission, such as a three-body break-up mechanism, will produce enhanced yields superimposed on the exponential decrease of the Poisson-like shapes at large ΔZ values as shown previously for ^{32}S induced reactions at 10 MeV/nucleon bombarding energies [28]. The data of the individual missing charges of Fig.8 are furthermore reasonably well reproduced by a statistical model calculation that will be presented later in this section.

An average charge-deficit value of $< \Delta Z > = 1.74$ is then obtained when only the fully-damped events are taken into account. This value is appreciably larger than the one measured for the same reaction at E_{lab} = 200 MeV [2,3] $< \Delta Z > = 0.96$. This result

confirms that the charge deficit increases linearly with the cm. bombarding energy and thus with the total excitation energy available in the composite system [22] and indicates that the emission process is the statistical evaporation from equilibrated nuclei. To illustrate this the average charge-deficit values obtained in the present work along with a collection of other data taken from the literature [21,22] have been plotted against the cm. bombarding energy in Fig.9 as proposed by Winkler et al. [22]. The two $^{35}Cl+^{12}C$ data points are shown as stars, whereas the point measured for the $^{35}Cl+^{24}Mg$ reaction [29,30] is shown as an open cross. The linear dependence is fitted by the following relationship :

$$< \Delta Z > = 0.048\ (E_{c.m.} - 37.12),$$

where the cm. energy is in units of MeV. This behaviour is shown as a straight line in Fig.9. An energy threshold of about 37 MeV is found for the emission of light-charged particles and an excitation energy increase of 21 MeV is required on average for the emission of one unit of particle charge in qualitative agreement with previous analyses [22,28]. Similar conclusions have also been reached from inclusive measurements of ER mass distributions [31] and from exclusive measurements on the decay of projectile-like fragments in the intermediate energy domain [32]. These results suggest that the emission occurs as a statistical evaporation from equilibrated nuclei.

In summary, the present charge-deficit results are consistent with a statistical decay of binary fragments and follow the proposed systematic for this behaviour quite well, in contrast to the data of [26,27]. The absence of ternary events in the present measurement is consistent with results from ^{32}S induced reactions where evidence of three-body processes is only seen at incident energies higher than 10 MeV/nucleon [28]. It can be surmised that, in the present experiment, the inclusive cross sections measured for the lightest Z fragments ($Z \leq 12$) arise from a fully-damped binary process, such as FF, followed by a sequential emission of light-charged particles and neutrons. In the subsequent discussion we will consider these fragments as FF fragments.

In Fig.10 the strongest FF channels for the $^{35}Cl+^{12}C$ reaction measured at E_{lab} = 280 MeV in this work are presented individually for each element along with the previously

published data [1,2,39] between E_{lab} = 150 MeV and 200 MeV. This provides experimental elemental excitation functions to which statistical-model calculations can be compared.

The FF cross sections rise rapidly with increasing bombarding energies and then more slowly at higher energies. This behaviour is a characteristic signature of a statistical CN emission. Therefore it is not surprising that the experimental elemental excitation functions are very well explained in the framework of statistical model calculations [6,7] as shown by the results given in Fig.4 for two types of models.

The first model is based upon the transition-state theory [6] for which the fission width is assumed to depend on the available phase space of the saddle point. The second model corresponds essentially to an extension of the Hauser-Feshbach formalism [7,8] which treats γ-ray emission, light-particle (n, p, and α) evaporation and FF as the possible decay channels in a single and equivalent way. The Extended Hauser-Feshbach Method (EHFM) assumes that the fission probability is proportional to the available phase space at the scission point. Both calculations start with the CN formation hypothesis and then follows the system by first chance binary fission or light-particle emission and subsequent light-particle and/or photon emission. In the following the full procedure of EHFM, including secondary emission, will be called EHFM+CASCADE. For instance it is clearly shown from the EHFM calculations of Fig.8 that the sequential emission plays an important role in the deexcitation scheme.

In the transition-state model the geometry of the saddle point, including the role of the fragment deformation, is fully determined by macroscopic energy calculations. The mass-asymmetric fission barriers are calculated following the procedure outlined in the liquid drop model of Sierk [33] in order to incorporate effects resulting from finite range of the nuclear interaction and the diffuseness of the nuclear surface [34]. Both FF and ER yields are calculated using a modified version of the code CASCADE [35]. The effect of light-particle emission from the fission fragments (significant at high excitation energy as shown previously) on the observed element distributions was simulated using the binary-decay option of LILITA [17]. The transition-state model is an *ab initio* calculation based on our current best understanding of the macroscopic energies of light systems. This calculation

leads to certain results which appear to agree well with experiment [6]. In the following the full transition-state model calculations with sequential decay will be labelled as TSM.

The EHFM is an alternative approach using the phase space at the scission point to determine relative probabilities. In the EHFM calculations the scission point can be viewed as an ensemble of two, near-touching spheres which are connected with a neck degree of freedom. The value of the neck length parameter (or separation distance) $s = 3.0 \pm 0.5$ fm is chosen, as is commonly adopted in the literature [2,36–38] for the mass region of interest. The large value of s used for the neck length mimics the finite-range and diffuse-surface effects [6] of importance for the light-mass systems [19,34] and, as a consequence, this makes the scission configurations closely resemble the saddle configurations of the Sierk model [33]. A systematic study of a large number of systems [7,8] allows the parameters of the model to be fixed so as to achieve good agreement with the experimental results. Recent studies [8] in the framework of EHFM have led to scission configurations being deduced for the lighter systems being studied [8].

In EHFM+CASCADE the calculations are performed by assuming first chance fission which is then followed by a sequential emission of light-charged particles and neutrons from the fragments. Second chance fission is found, as expected, to be negligible in this mass region and, therefore, pre-scission emission was not taken into account in the decay process. The results of the calculated post-scission emission is illustrated in Fig.8 by a comparison with the experimental data. EHFM+CASCADE is capable of predicting not only the fission fragment and ER yields, but also the FF kinetic-energy distributions and their TKE mean values as shown in Figs. 2 and 3 respectively.

The input parameters of the two models are basically the same. In each case, the diffuse cut-off approximation has been assumed for the fusion partial-wave distribution using a diffuseness parameter of A = $1\hbar$ and L_{crit} values as calculated from the experimental total fusion cross sections given in the previous section or taken from previous measurements [1–3] at the lower bombarding energies.

The predictions of both approaches can be compared to fully-damped yield data in Figs.4

and 10. A disagreement between the model calculations and the experimental results as seen in Fig.4 corresponds to a too large observed mass asymmetry. However, the predictions of EHFM+CASCADE and TSM displayed in Fig.10 provide a quite satisfactory agreement of the general trends of the $^{35}Cl+^{12}C$ experimental data over the whole energy range explored. This might be a good indication of the validity of the hypothesis that the saddle-point shape almost coincides with the scission point configurations in this mass region [6–8].

The mass-asymmetric-dependent fission barriers of Sierk [33], which are central to the success of the TSM calculations [6], appear to be appropriate in a first-order analysis of the experimental $^{35}Cl+^{12}C$ FF excitation functions. Although more detailed theoretical approaches to the fission barriers will be needed in this mass region along with other excitation-function measurements for "sub-threshold" bombarding energies, the extracted "fission thresholds" appear to be quite well understood within a systematic framework which has been recently established [19]. Experimental studies are being currently undertaken in order to precisely determine the angular momentum dependence of the mass-asymmetric fission barriers of light nucleus in this mass region.

To summarize, the measured yields of fully energy-damped binary fragments from the $^{35}Cl+^{12}C$ reaction at 280 MeV have been analysed as arising from a fission process, in accordance with previous findings at lower incident energies [1–6]. The coincident data do not show any evidence for the occurrence of three-body processes, in contrast to recent observations for a similar system at a comparable energy. The "charge deficits" found in the measurement are well described by a complete Extended Hauser-Feshbach statistical-model calculation which takes into account the post-scission light-particle evaporation and, thus, can be well understood a-s the result of the sequential decay of hot binary fragments. This is in agreement with the systematic behaviour that has been established for other reactions studied at bombarding energies below 10 MeV/nucleon. The experimental $^{35}Cl+^{12}C$ elemental FF excitation functions have been successfully described within the framework of the statistical model based on either the saddle point picture or the scission point pic-

ture. The mass-asymmetric-dependent fission barriers needed in the transition-state model calculations are found to be appropriate in this mass region.

ACKNOWLEDGMENTS

The authors wish to thank the Post-accelerated Tandem Service at Saclay for the kind hospitality and the technical support. S. Leotta and S. Reito from Catania are also warmly thanked for their assistance during the set-up of all of the experiments. One of us (S. J. S.) would like to acknowledge the NSF for support within the framework of a CNRS/NSF collaboration program and the U.S. Department of Energy for support under the Contract Number DE-FG02-89ER40508.

REFERENCES

[a] On leave from the Faculty of Textile Science and Technology, Shinshu University, Ueda, Nagano, 386, Japan, as an Overseas Research Scholar of Japan.

[b] Present Address: Department of Chemistry, University of Rochester, Rochester NY 14627, USA.

[c] Permanent Address: Département de Physique, Université de Nice-Sophia-Antipolis, F-06034 Nice, France.

[d] Present Address: Faculté des Sciences, Université Hassan II, Casablanca, Maroc.

[e] Present Address: GANIL, F-14021 Caen Cedex, France.

[1] C. Beck, B. Djerroud, B. Heusch, R. Dayras, R.M. Freeman, F. Haas, A. Hachem, J.P. Wieleczko, and M. Youlal , Z. *Phys.* **A334**, 521 (1989).

[2] C. Beck, B. Djerroud, F. Haas, R. M. Freeman, A. Hachem, B. Heusch, A. Morsad, Y. Abe, A. Dayras, J.P. Wieleczko, T. Matsuse, and S.M. Lee, Z. *Phys.* **A343**, 309 (1992).

[3] B. Djerroud, Ph.D. Thesis, Strasbourg University, 1992, Report NO. CRN/PN 92/32, 1992.

[4] A. Ray, D. Shapira, J. Gomez del Campo, H.J. Kim, C. Beck, B. Djerroud, B. Heusch, D. Blumenthal, and B. Shivakumar, *Phys.* Rev. **C44**, 514 (1991).

[5] C. Beck, B. Djerroud, F. Haas, R. M. Freeman, A. Hachem, B. Heusch, A. Morsad, and M. Vuillet-A-Cilles , *Phys.* Rev. **C47**, 2093 (1993).

[6] S.J. Sanders, *Phys. Rev.* **C44**, *2676 (1991).*

[7] T. Matsuse, S.M. Lee, Y.H. Pu, K.Y. Nakagawa, C. Beck and T. Nakagawa, in Procced-

ings of the International Symposium Towards a *Unified Picture of Nuclear Dynamics* , Nikko 1990, AIP Conference Proceedings 250, 112 (1991), edited by Y. Abe, S.M. Lee and F. Sakata.

[S] T. Matsuse, R. Nouicer, D. Mahboub and C. Beck, in preparation.

[9] Sl. Cavallaro, C. Beck, E. Berthoumieux, R. Dayras, E. De Filippo, G. Di Natale, B. Djerroud, R.M. Freeman, A. Hachem, F. Haas, B. Heusch, G. Lanzanò, R. Legrain, D. Mahboub, A. Morsad, A. Pagano, E. Pollacco, S.J. Sanders, and M.L. Sperduto, *Nucl. Phys.* **A583**, 161 (1995).

[10] C. Beck, Y. Abe, N. Aissaoui, B. Djerroud and F. Haas, *Phys.* Rev. **C49**, 2618 (1994); *Nucl. Phys.* **A583**, 269 (1995).

[11] A. Moroni, I. Iori, Li Zu Yu, G. Prete, G. Viesti, F. Gramegna, and .4. Dainelli, *Nucl. Instr. Meth.* **A225**, 57(1984)

[12] S.B. Kaufman, E.P. Steinberg, B.D. Wilkins, J. Unik, A.J. Gorski, and M.J. Fluss, *Nucl. Instr. Meth.* 115, 47 (1974)

[13] R.J. Charity, D.R. Bowman, Z.H. Liu, R-J. McDonald, M.A. McMahan, G.J. Wozniak, L.G. Moretto, S. Bradley, W.L. Kehoe, and A.C. Mignerey, *Nucl. Phys.* **A476**, 516 (1988).

[14] V.E. Viola, K. Kwiatkowski, and M. Walker, *Phys. Rev.* **C31**, 1550 (1985).

[15] W.W. Wilcke, J.R. Birkelund, H.J. Wollersheim, A.D. Hoover, J.R. Huizenga, W.U. Schröder, and L.E. Tubbs, *Atomic Data* and *Nuclear* Data *Tables* 25.389 (1980).

[16] H. Morgenstern, W. Bohne, W. Galster, K. Grabisch, and A. Kyanowski, *Phys. Rev. Lett. 53, 1104 (1984).*

[17] J. Gomez del Campo, and R.G. Stockstad, Oak Ridge National Laboratory Technical Report ORNL-TM-7295,1981

[18] S. Ayik, S. Shapira, and B. Shivakumar, *Phys. Rev.* **C38**, 2610 (1988).

[19] c. Beck, and A. Szanto de Toledo, *Phys.* Rev. **C53**, (1996), in press.

[20] R. Novotny, U. Winkler, D. Pelte, H. Sann, and U. Lynen, *Nucl. Phys.* **A341**, 301 (1980).

[21] D. Pelte, U. Winkler, R. Novotny, and H. Gräf, *Nucl. Phys.* **A371**, 454 (1981).

[22] U. Winkler, R. Giraud, H. Gräf, A. Karbach, R. Novotny, D. Pelte, and G. Strauch, *Nucl. Phys.* **A371**, 477 (1981).

[23] U. Winkler, B. Weissman, M. Bühler, A. Gorks, R. Novotny, and D. Pelte, *Nucl. Phys.* **A425**, 573 (1984).

[24] D. Pelte, U. Winkler, J. Pochodzalla, M. Bühler, A. Gorks, and B. Weissman, *Nucl. Phys.* **A438**, 582 (1985).

[25] D. Pelte, U. Winkler, M. Bühler, B. Weissman, A. Gobbi, K.D. Hildenbrand, H. Stelzer, and R. Novotny, *Phys. Rev.* **C34**, 1673 (1986).

[26] G. Vannini, I. Massa, L. Lavagnini, P. Boccaccio, L. Vannucci, R.A. Ricci, I. Iori, J.P. Coffin, P. Fintz, M. Gonin, G. Guillaume, B. Heusch, F. Jundt, A. Malki, F. Rami, and P. Wagner , *Europhys. Lett.* 7(4), 311 (1988).

[27] P. Boccaccio, P.K. Mwose, L. Vannucci, M. Bettiolo, R.A. Ricci, W. Augustyniak, I. Massa, G. Vannini, J.P. Coffin, P. Fintz, G. Guillaume, B. Heusch, F. Jundt, F. Rami, and P. Wagner, *Nuovo Cimento* **106A**, 379 (1993); P. Boccaccio, M. Bettolio, R. Doná, L. Vannucci, R.A. Ricci, G. Vannini, L. Massa, J.P. Coffin, P. Fintz, G. Guillaume, F. Jundt, F. Rami, and P. Wagner, Z. *Phys.*, *(1996),* in press.

[28] J. Betz, H. Graff, R. Novotny, D. Pelte, and U. Winkler, *Nucl. Phys.* **A408**, 150 (1983).

[29] C. Beck, D. Mahboub, R. Nouicer, B. Djerroud, R.M. Freeman, F. Haas, A. Hachem, Sl. Cavallaro, E. De Filippo, E. Di Natale, G. Lanzanò, A. Pagano, M. Sperduto, R.

Dayras, E. Berthoumieux, R. Legrain and, E. Pollaco, Proc. of the XXXIII Intern. Winter Meeting, Bormio, 1995, ed. I. Iori, Ricerca Scientific ed Educazione Permanence Supp. 101, 127 (1995).

[30] R. Nouicer, C. Beck, D. Mahboub, B. Djerroud, R.M. Freeman, A. Hachem, T. Matsuse, Sl. Cavallaro, E. De Filippo, G. Lanzanò, A. Pagano, M.L. Sperduto, R. Dayras, E. Berthoumieux, R. Legrain and E. Pollacco, Z. *Phys.* , *(1996)* to be submitted.

[31] H. Morgenstern, W. Bohne, K. Grabisch, H. Lehr, and W. Stöffler, *Z. Phys.* **A313**, 39 (1983).

[32] L. Beaulieu, M. Samri, B. Djerroud, G. Auger, G.C. Ball, D. Doré, A. Galindo-Uribarri, P. Gendron, E. Hagberg, D. Horn, E. Jalbert, R. Laforest, Y. Larochelle, J.L. Laville, O. Lopez, E. Plagnol, J. Pouliot, R. Regimbart, R. Roy, J.C. Steckmeyer, C. St-Pierre, and R.B. Walker, *Phys. Rev.* **C51**, 3492 (1995).

[33] A.J. Sierk, *Phys. Rev.* **C33**, 2039 (1986).

[34] H.J. Krappe, J.R. Nix and A.J. Sierk, *Phys. Rev.* **C20**, 992 (1979).

[35] F. Pühlhofer, *Nucl. Phys.* **A280** ,267 (1977).

[36] J.R. Natowitz, M.N. Eggers, P. Gonthier, K. Geoffroy, R. Hanus, C. Towsley and K. Das, *Nucl. Phys.* **A277**, 477 (1977).

[37] N. Van Sen, R. Darves-Blanc, J.C. Gondrand and F. Merchez, *Phys. Rev.* **C27**, 194 (1983).

[38] Y.H. Pu, S.M. Lee, S.C. Jeong, H. Fujiwara, T. Mizota, Y. Futami, T. Nakagawa, H. Ikezoe and Y. Nagame, Z. *Phys.* **A353**, 387 (1996).

[39] W. Yokota, T. Nakagawa, M. Ogihara, T. Komatsubara, Y. Fukuchi, K. Suzuki, W. Galster, Y. Nagashima, K. Furuno, S.M. Lee, T Mikumo, K . Ideno, Y . Tomita, H . Ikezoe, Y. Sugiyama, and S. Hanashima, Z. *Phys.* **A333**, 379 (1989).

FIGURES

Fig.1 : Two dimensional charge versus velocity contour plot of the fragment invariant cross sections measured for $^{35}Cl+^{12}C$ at E_{lab} = 278 MeV at θ_{lab} = - 7°. The dotted-dashed line corresponds to the CN recoil velocity whereas the dashed line is the velocity of the projectile. The solid lines have been calculated using the Viola systematic as discussed in the text.

Fig.2 : Experimental (solid lines) inclusive energy spectra measured for $^{35}Cl+^{12}C$ at E_{lab} = 278 MeV at θ_{lab} = - 7°. The dashed lines are the results of the EHFM+CASCADE calculations discussed in the text whereas the black histograms are ER energy distributions as calculated by the Monte Carlo code LILITA. The results of the calculations have been arbitrarily normalized to the data for the sake of clarity.

Fig.3 : Angular dependence of the TKE values of the fully-damped fragments measured for $^{35}Cl+^{12}C$ at E_{lab} = 280 MeV. Averaged TKE values are plotted as a function of the atomic number in the insert along with DI model (dashed line) and EHFM+CASCADE (solid line) calculations discussed in the text.

Fig.4 : $^{35}Cl+^{12}C$ elemental distribution (points) measured at E_{lab} = 280 MeV compared to two statistical model calculations discussed in the text. The open and full histograms correspond to EHFM+CASCADE and TSM calculations respectively.

Fig.5 : $^{35}Cl+^{12}C$ experimental angular correlations between two heavy fragments with charges $Z_1 \geq 5$ and $Z_2 \geq 5$ measured at E_{lab} = 278 MeV. The first fragment is detected at a fixed angle θ_1 = - 7° whereas the second one is detected at a variable angle θ_2. The dashed lines are plotted as a guide to the eye.

Fig.6 : Cross sections for coincidence events between two heavy fragments with charge Z_1 and 2_2 measured respectively for $^{35}Cl+^{12}C$ at E_{lab} = 278 MeV for the indicated angle settings for which θ_1 = - 7°. The size of the squares is linearly proportional to the relative intensity of the pair. The solid lines correspond to binary reactions without light-charged-particle emission from the fragments.

Fig.7 : Summed charge deficits as measured for $^{35}Cl+^{12}C$ at E_{lab} = 278 MeV for the indicated angle settings for which 19_1 = -7°. The solid lines are Poisson distribution fits as explained in the text.

Fig.8 : Individual charge deficits (solid histograms) as measured for $^{35}Cl+^{12}C$ at E_{lab} = 278 MeV for each charge with the chosen angle setting. The dashed histograms are the results of the EHFM+CASCADE calculations discussed in the text.

Fig.9 : Systematic of the measured charge deficits. The solid line is the result of a least-square fit procedure discussed in the text. The stars and open cross symbols correspond to the data presented in this work, whereas the other symbols are results taken from other works.

Fig.10 : Experimental $^{35}Cl+^{12}C$ FF elemental excitation functions (points) compared with the TSM calculations (solid lines) and EHFM+CASCADE calculations (dashed lines) respectively.

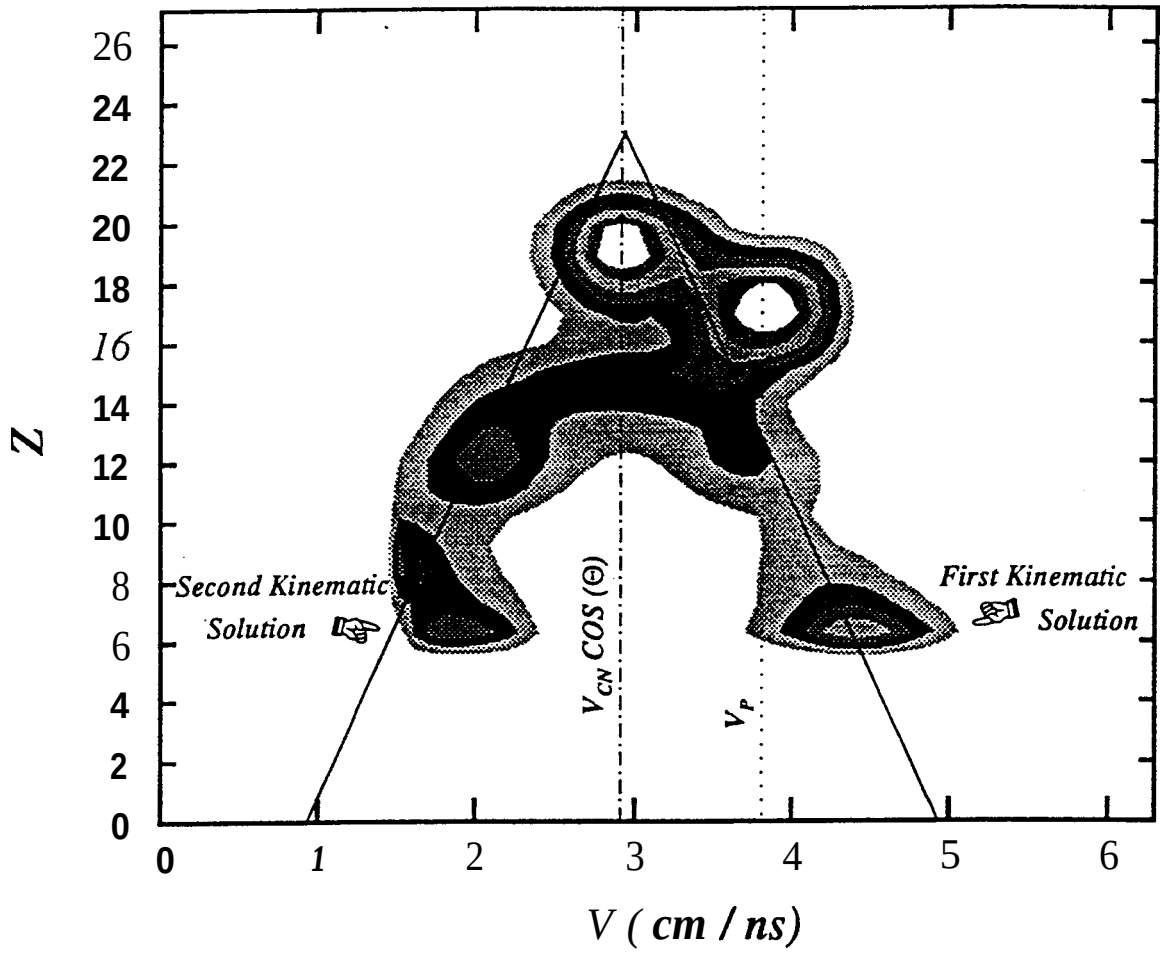

Fig. 1: $^{35}Cl + ^{12}C$ asymmetrical fission excitation functions
C. Beck et al.

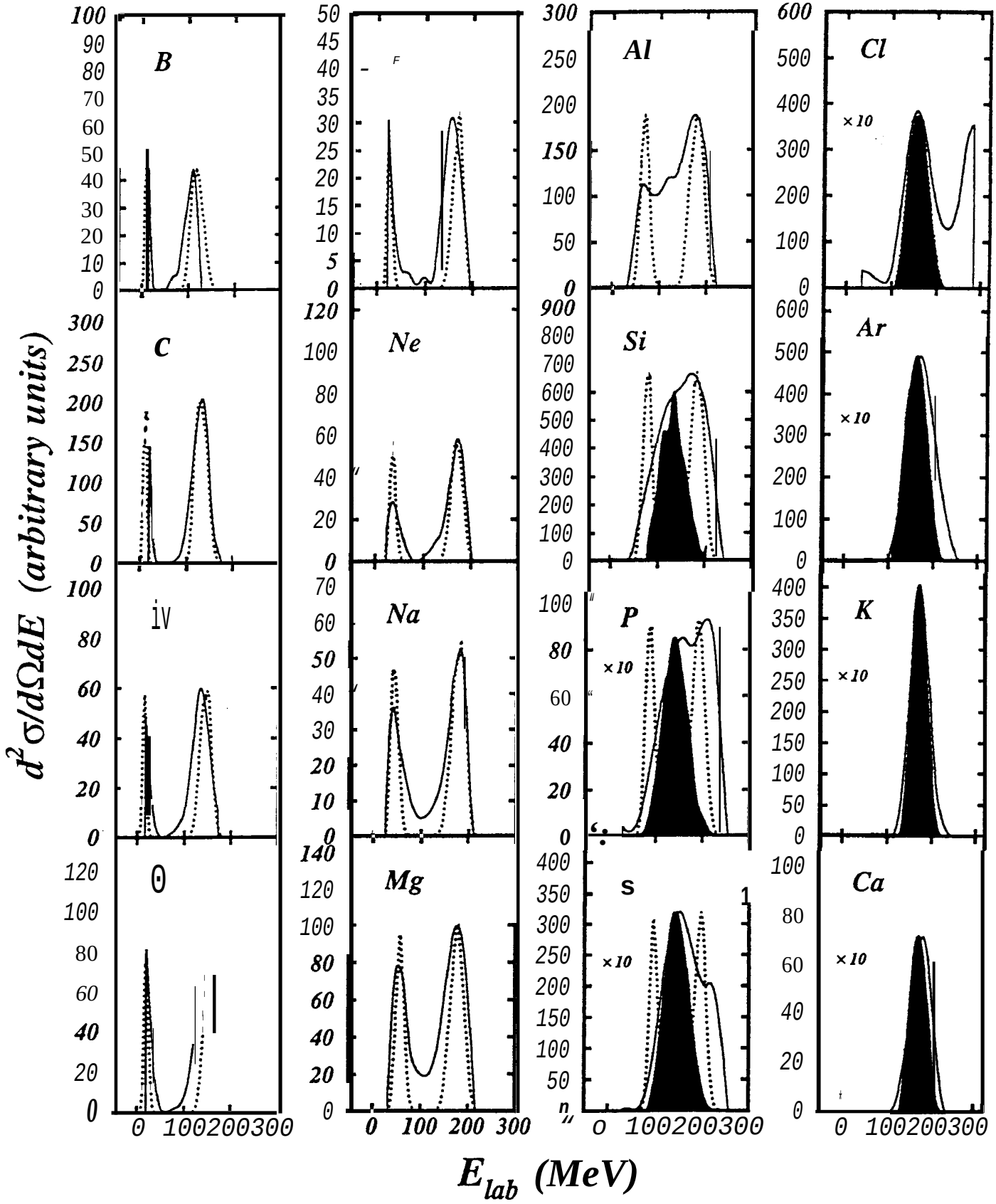

Fig. 2 : $^{35}Cl + ^{12}C$ asymmetrical fission excitation functions

C. Beck et al.

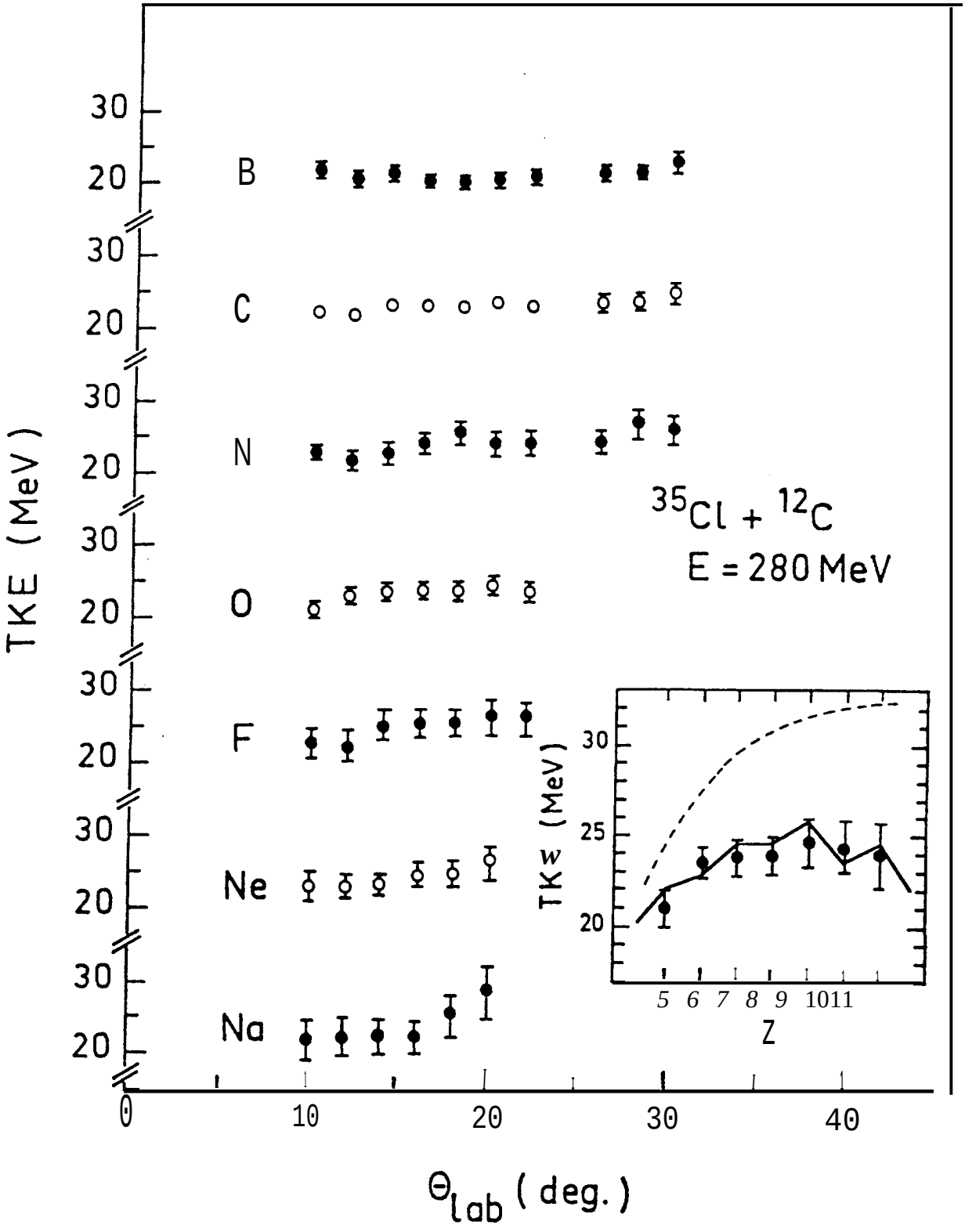

Fig. 3 : $^{35}Cl + ^{12}C$ asymmetrical fission excitation functions

C. Beck et al.

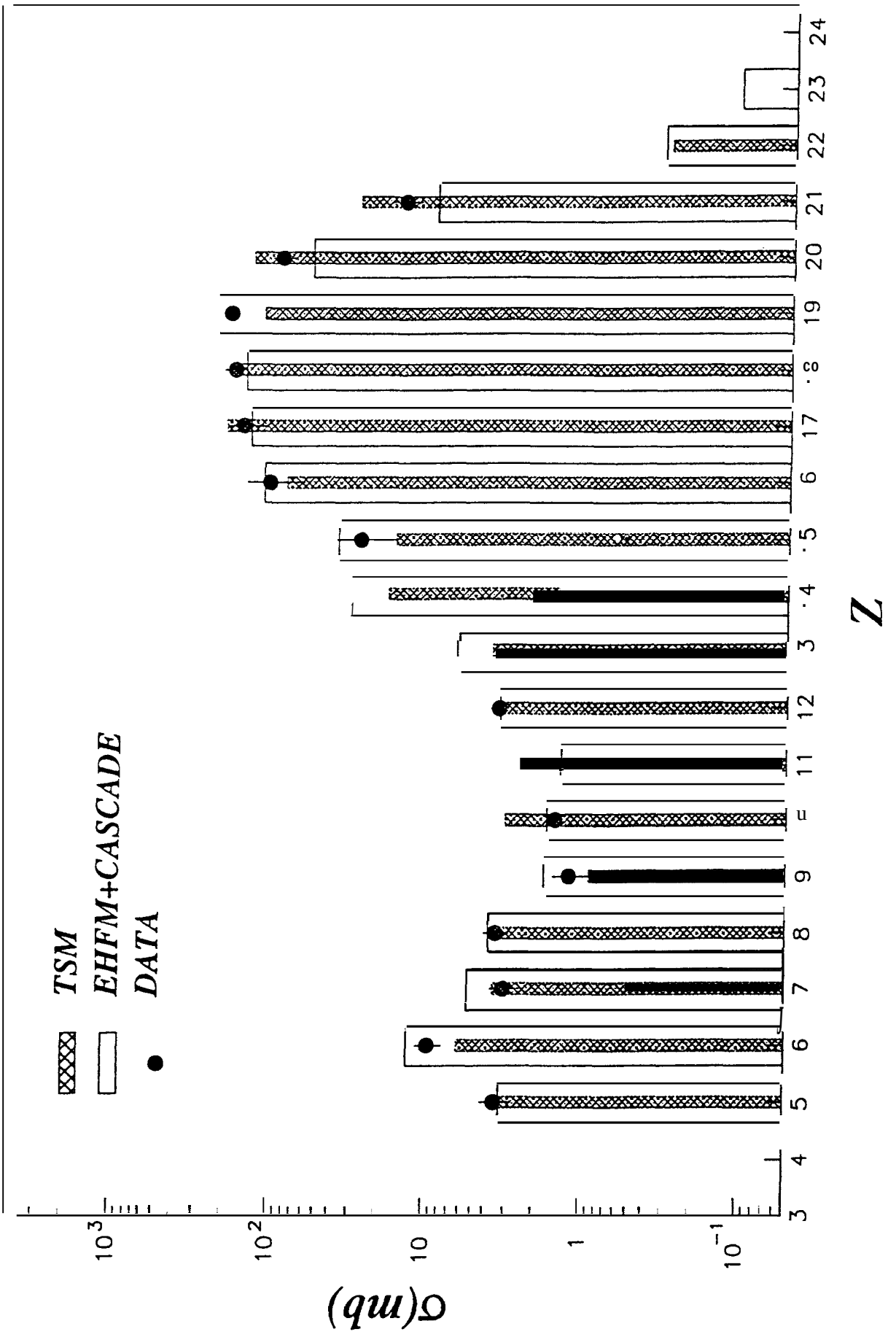

Fig. 4 : $^{35}Cl + ^{12}C$ asymmetrical fission excitation functions
C. Beck et al.

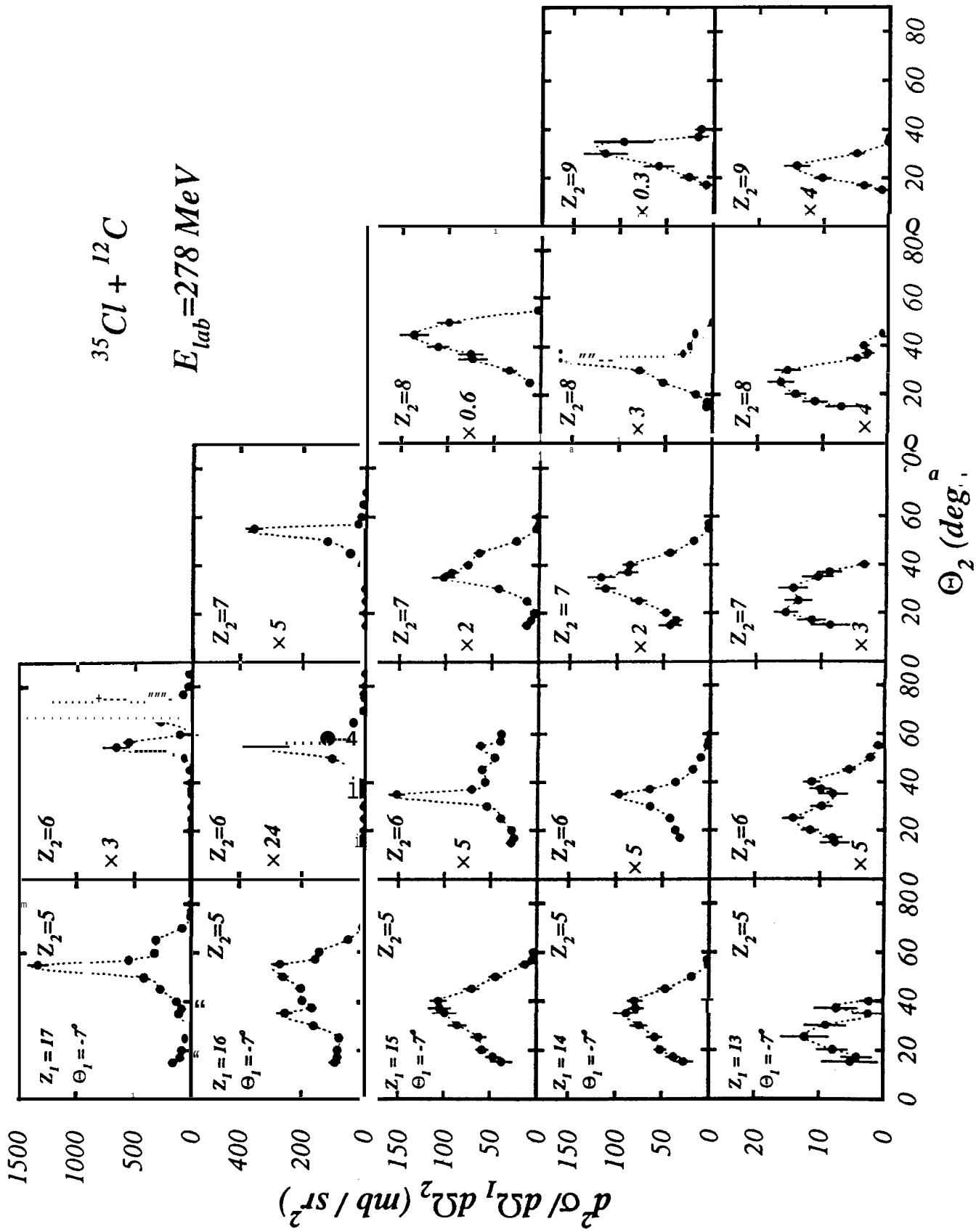

Fig. 5 : $^{35}Cl + ^{12}C$ asymmetrical fission excitation functions

C. Beck et al.

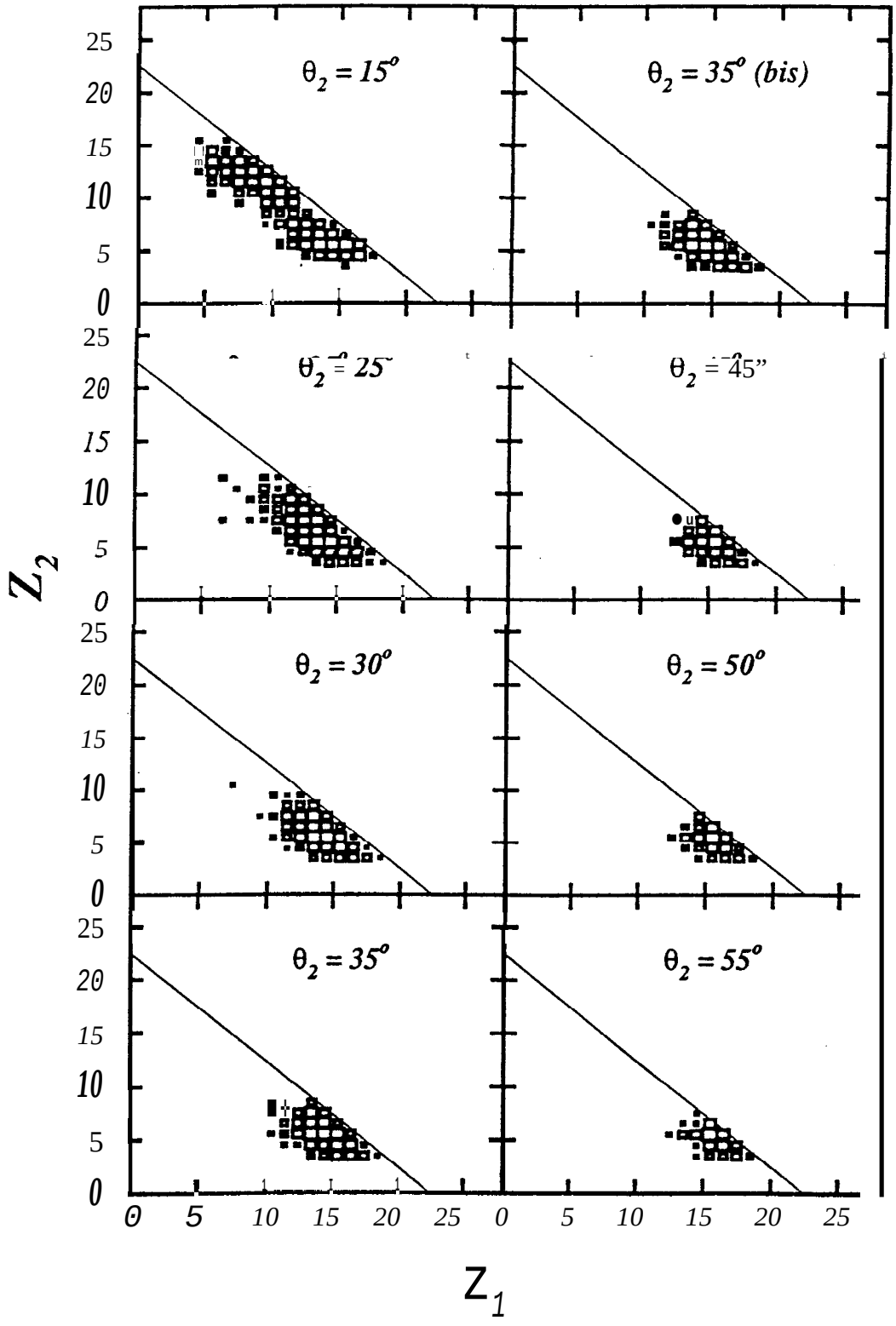

Fig. 6 : $^{35}Cl + ^{12}C$ asymmetrical fission excitation functions

C. Beck et al.

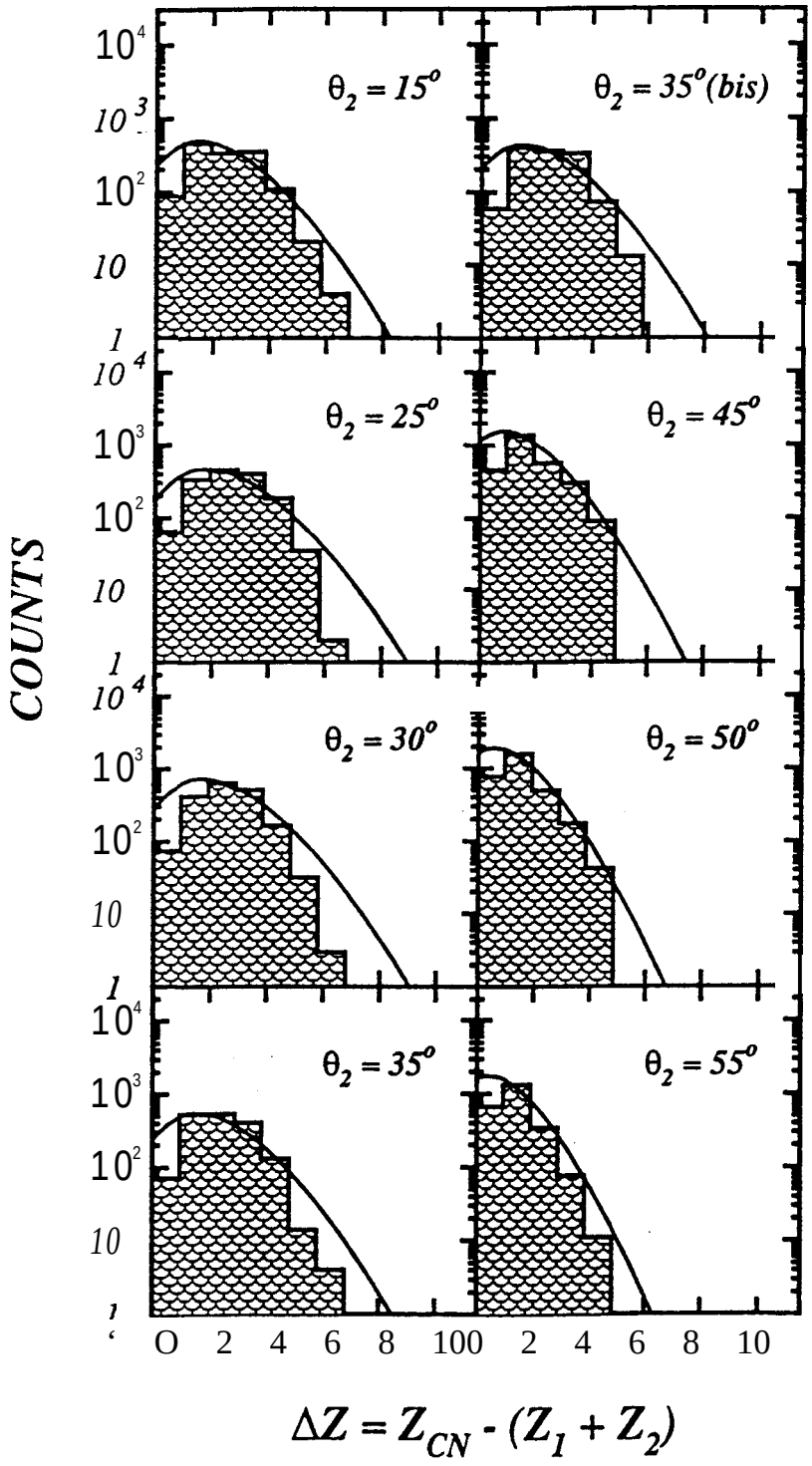

Fig. 7 : $^{35}Cl + ^{12}C$ asymmetrical fission excitation functions
C. Beck et al.

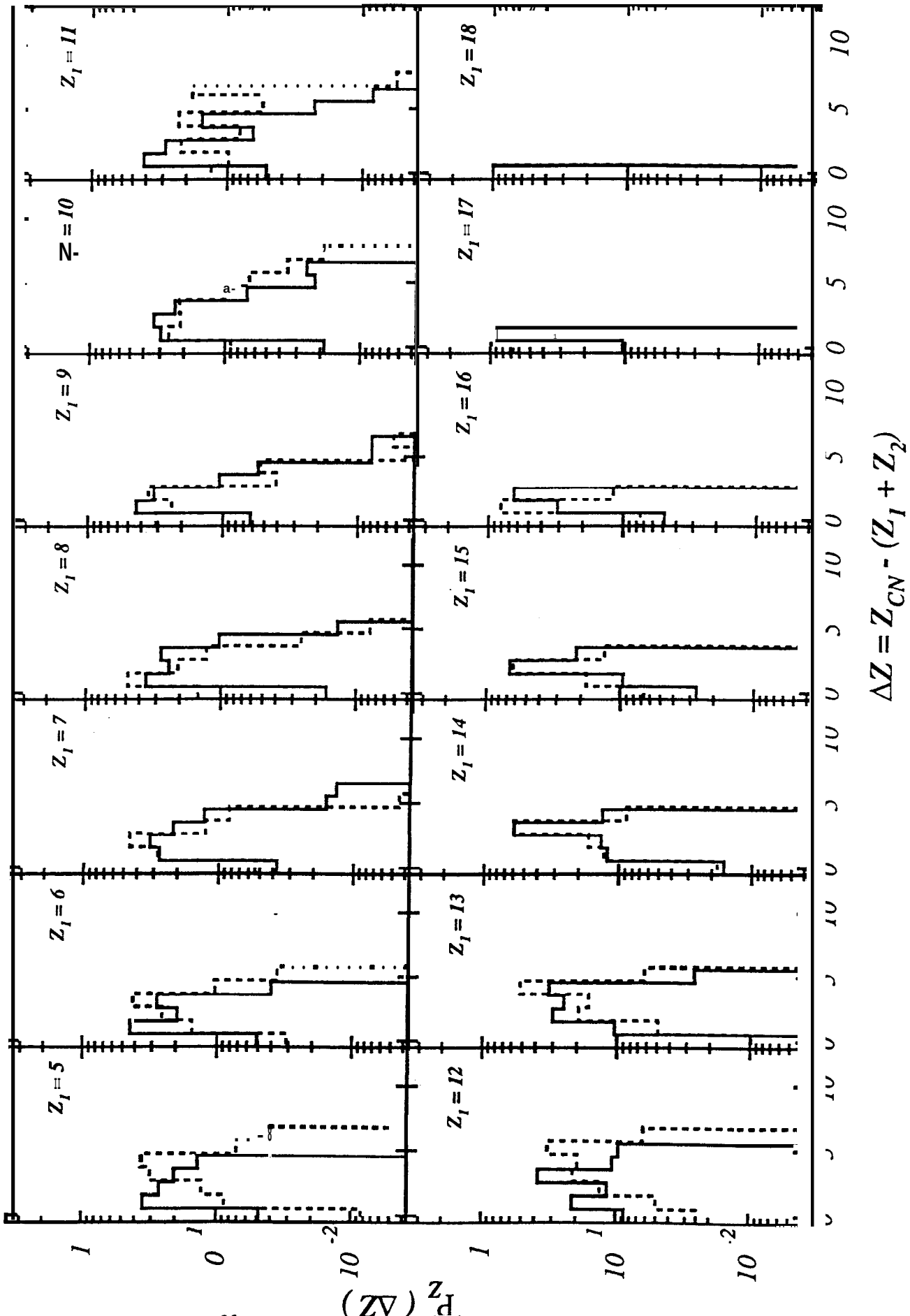

Fig. 8 : $^{35}Cl + ^{12}C$ asymmetrical fission excitation functions

C. Beck et al.

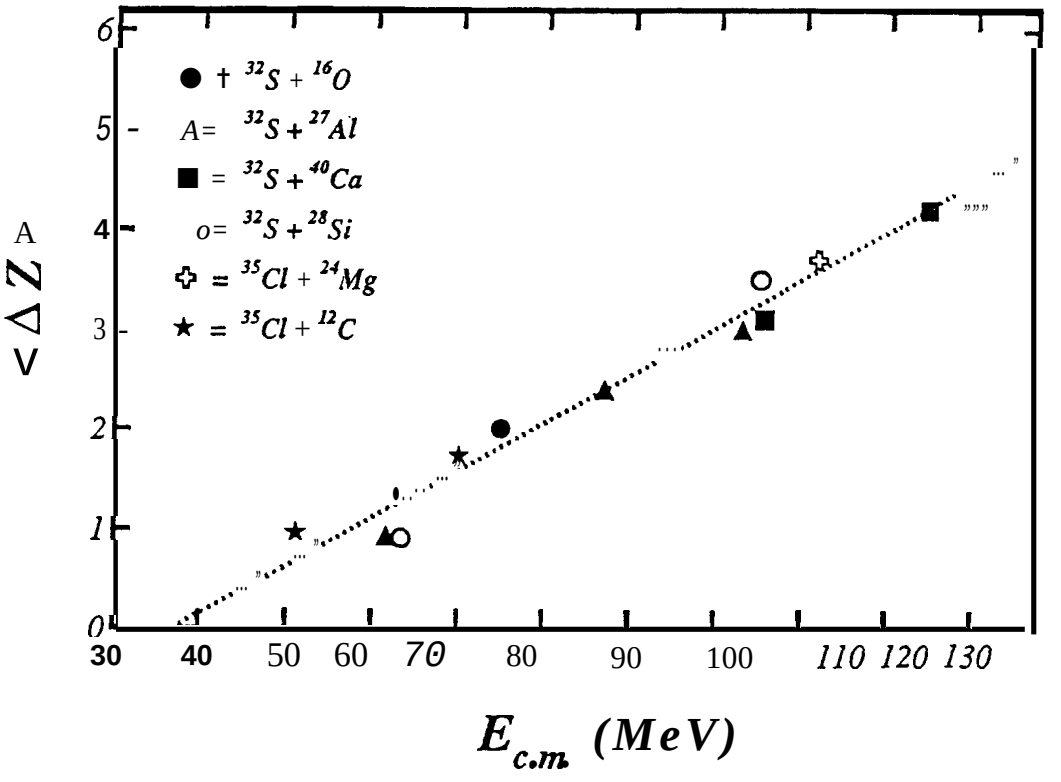

Fig. 9 : $^{35}Cl + ^{12}C$ asymmetrical fission excitation functions

C. Beck et al.

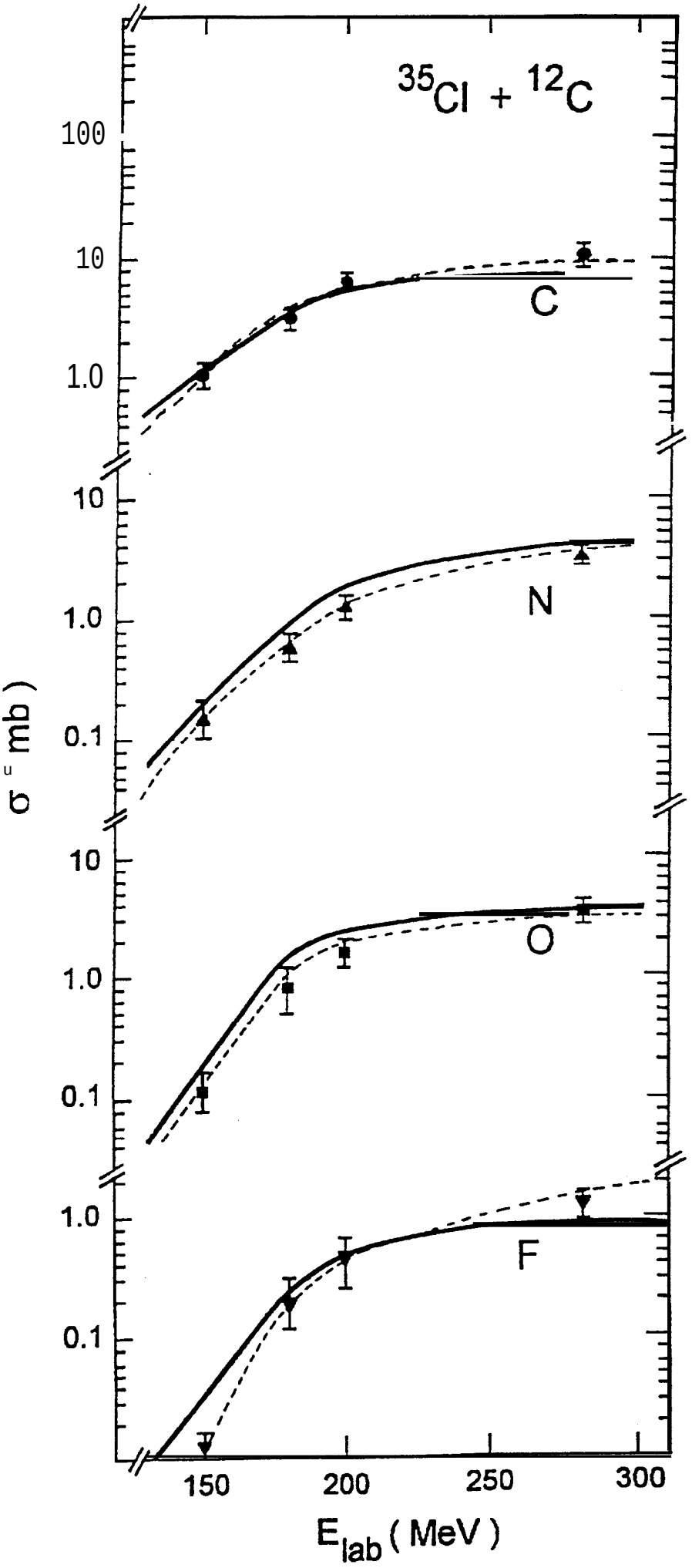

Fig. 10 : $^{35}Cl + ^{12}C$ asymmetrical fission excitation functions
C. Beck et al.